





High-order harmonic generation using quasi-phase matching and two-color pump in the plasmas containing molecular and alloyed metal sulfide quantum dots

Cite as: J. Appl. Phys. **126**, 193103 (2019); <https://doi.org/10.1063/1.5124139>

Submitted: 12 August 2019 . Accepted: 04 November 2019 . Published Online: 15 November 2019

Rashid A. Ganeev , Ganjaboy S. Boltaev , Vyacheslav V. Kim , Mottamchetty Venkatesh, Andrey I. Zvyagin, Michail S. Smirnov, Oleg V. Ovchinnikov, Michael Wöstmann, Helmut Zacharias, and Chunlei Guo 



View Online



Export Citation



CrossMark

Lock-in Amplifiers
... and more, from DC to 600 MHz



High-order harmonic generation using quasi-phase matching and two-color pump in the plasmas containing molecular and alloyed metal sulfide quantum dots

Cite as: J. Appl. Phys. **126**, 193103 (2019); doi: [10.1063/1.5124139](https://doi.org/10.1063/1.5124139)

Submitted: 12 August 2019 · Accepted: 4 November 2019 ·

Published Online: 15 November 2019



Rashid A. Ganeev,^{1,2,3,a)} Ganjaboy S. Boltaev,^{1,3} Vyacheslav V. Kim,^{1,3} Mottamchetty Venkatesh,¹ Andrey I. Zvyagin,² Michail S. Smirnov,^{2,4} Oleg V. Ovchinnikov,² Michael Wöstmann,⁵ Helmut Zacharias,⁵ and Chunlei Guo^{1,6,b)}

AFFILIATIONS

¹The Guo China-US Photonics Laboratory, State Key Laboratory of Applied Optics, Changchun Institute of Optics, Fine Mechanics and Physics, Chinese Academy of Sciences, Changchun 130033, China

²Faculty of Physics, Voronezh State University, 1 University Square, Voronezh 394018, Russia

³Department of Physics, American University of Sharjah, PO Box 26666, Sharjah, UAE

⁴Scientific and Educational Center "NanoBioTech", Voronezh State University of Engineering Technologies, Voronezh 394017, Russia

⁵Center for Soft Nanoscience, University of Münster, 48149 Münster, Germany

⁶The Institute of Optics, University of Rochester, Rochester, New York 14627, USA

a)rashid_ganeev@mail.ru

b)guo@optics.rochester.edu

ABSTRACT

As high-order harmonic emitters, quantum dots are produced through laser-induced plasmas. Subsequently, we generate high-order harmonics with 800-nm and 30-fs pulses from laser-produced plasmas containing quantum dots of different metal sulfides (Ag_2S , CdS , and $\text{Cd}_{0.5}\text{Zn}_{0.5}\text{S}$). The high-order harmonic generation is analyzed using different approaches, including two-color (800 nm + 400 nm) pump, application of alloyed quantum dots, and quasiphase matching of interacting waves. We discuss the self-phase modulation induced splitting of harmonics, the difference in the application of thick and thin crystals for second harmonic (400 nm) emission during two-color pumping of the quantum dot plasma, the spatial modulation of the quantum dot plasma for quasiphase matching, and the comparison of harmonic yields from monomer and quantum dot plasmas. This study allows us to determine the mechanisms of coherent extreme ultraviolet radiation generation using a few nanometer-sized emitters as well as optimal methods for further enhancing the high-order harmonic generation efficiency.

Published under license by AIP Publishing. <https://doi.org/10.1063/1.5124139>

I. INTRODUCTION

Quantum dots (QDs) play an important role in different technological fields. One interesting application is the formation of QD-containing media for the frequency conversion of ultrashort laser pulses from the IR toward the extreme ultraviolet range. The application of aggregated species for the high-order harmonic generation (HHG) allows the generation of coherent short-wavelength

sources of radiation and serves as a medium for an intensity enhancement of the extreme ultraviolet pulses. Typically, gas and plasma media are used as the surrounding environment for clusters, QDs, nanoparticles, microparticles, and large aggregates of atoms. Small-sized aggregates subject to intense laser pulses produce a strong low-order nonlinear optical response (e.g., nonlinear refraction and nonlinear absorption), as well as the emission of coherent extreme ultraviolet radiation through the harmonic generation.^{1–5}

Previous studies of the HHG from such objects were limited to the nanoclusters (Ar and Xe) being formed in high-pressure gas jets due to rapid cooling by adiabatic expansion, as well as to the relatively large nanoparticles ablated from the bulk surfaces.⁴

Recent studies of QDs have shown that particles with sizes of the order of a few nanometers can effectively generate high-order harmonics.⁷ HHG directly from QDs has not yet been studied theoretically, but a simulation of HHG from small clusters⁸ showed an increased HHG yield under the assumption of possible recombination of an electron on different atoms in the cluster. Though the mechanisms of the enhancement of the harmonic yield in such multiparticle systems are still debatable, several studies have confirmed the potential of these species for both enhancing the coherent extreme ultraviolet flux and understanding the fundamental aspects of laser-multiparticles interaction.^{1,2,6,9} The probable explanation for this HHG enhancement in gas and plasma multiparticle media is due to the larger recombination cross section for multiatomic particles leading to higher HHG efficiency. Additionally, the growing recombination of the accelerated electrons with the same or neighboring atoms, or with the multiatomic particles, may also be, to some extent, the reason of the observed growth of harmonic yield from clusters and nanoparticles.⁹

Laser-produced plasma produced on the surfaces of bulk materials attracts attention due to various processes occurring during the harmonic generation in this medium.^{10–19} Meanwhile, different aspects of the application of low-dimensional aggregates for efficient HHG in plasma media have yet to be analyzed. These unexplored concepts include (a) the application of two driving waves with different polarizations for the harmonic generation, (b) a modulation of the spatial shape of the aggregate-containing media to apply the quasiphase matching concept for harmonic enhancement in different ranges of the extreme ultraviolet, (c) a modification of the structure of aggregates for determining the role of morphology properties on the frequency conversion of infrared pulses in such structures, etc. In this connection, the laser-produced plasmas provide a wider range of options than the gaseous media for variation of the properties of aggregates-containing media.

In this paper, we analyze HHG from laser-produced plasmas containing QDs of metal sulfides using different approaches, including two-color pump, application of single and alloyed QDs, and quasiphase matching of interacting waves. This study allows us to determine the optimal methods for further enhancing HHG efficiency and analyzing the properties of harmonic emitters.

II. EXPERIMENTAL ARRANGEMENTS

Colloidal $\text{Cd}_{0.5}\text{Zn}_{0.5}\text{S}$ QDs were prepared through the mixing of CdBr_2 , ZnBr_2 , thioglycolic acid, and Na_2S at the ratio of 1:1:2:2 at 40 °C. The synthesized $\text{Cd}_{0.5}\text{Zn}_{0.5}\text{S}$ QDs were centrifuged with adding ethanol and acetone and then again dissolved in water. After cleaning the suspension obtained, the gelatin was added to this suspension. The concentration of QDs amounted to about 40% of the mass of gelatin. This method was based on the compatibility of synthesized colloidal QDs and gelatin, as well as the possibility of increasing the concentration of QDs during centrifugation in the presence of acetone. The mean sizes of $\text{Cd}_{0.5}\text{Zn}_{0.5}\text{S}$ QDs measured using transmission electron microscope (TEM) were 2 nm, while

the other species had mean sizes in the range of 1.7–2.0 nm (Ag_2S) and 3.0–3.2 nm (CdS). The optical spectra of the suspensions of these QDs were significantly blue-shifted with regard to the bulk materials of similar materials. The $\text{Cd}_{0.5}\text{Zn}_{0.5}\text{S}$, CdS , and Ag_2S QDs embedded in gelatin were prepared in the form of $5 \times 5 \times 3$ mm plates. The solid targets containing the mixtures of gelatin and synthesized samples of colloidal solutions of cadmium, cadmium-zinc, and silver sulfides were then ablated in a vacuum chamber using the cylindrical focusing optics to produce 5 mm long laser-produced plasmas where HHG was carried out. This method allowed the formation of plasmas containing a large amount of QDs leading to an enhancement of the harmonic yield with regard to the ablation of bulk materials of the same elemental components. We also used silver sulfide bulk targets with the same composition as the QDs to compare HHG in single atomic/ionic and QD species.

TEM image of deposited debris from bulk Ag_2S is shown in Fig. 1(a). No measurable nanoparticles were observed since the deposited debris presented a thin molecular film. These morphology studies confirmed that the emission of harmonics in that case occurred from the molecular components of the plasma rather than from the multiparticle associates aggregated during ablation of bulk silver sulfide at relatively mild conditions of ablation (i.e., at a fluence of the heating nanosecond pulses of $\sim 100 \text{ J cm}^{-2}$). This image was taken at optimal fluence for ablation of this target. The term “optimal” (as in any other cases) refers to the maximal yield of harmonics from laser-produced plasma. Stronger ablation of bulk Ag_2S caused a sharp decrease of the harmonic conversion efficiency, while no difference in the debris with the previous case was detected. Further enhancement of the fluence (above 250 J cm^{-2}) caused the appearance of large associates of silver sulfide (\sim a few micrometers) among the debris, probably caused by blast-induced evaporation of large bullets from the bulk surface. For comparison, we show the image of deposited Ag_2S QDs used during present HHG studies [Fig. 1(b)]. The sizes of deposited QDs were almost similar to those from the initial QDs.

Femtosecond laser pulses (800 nm, 30 fs, 1 kHz, Spectra Physics, Spitfire Ace) were employed for HHG during propagation at a distance of $\sim 200 \mu\text{m}$ above the target surface through the QD-containing laser-produced plasmas [Fig. 2(a)]. We used a

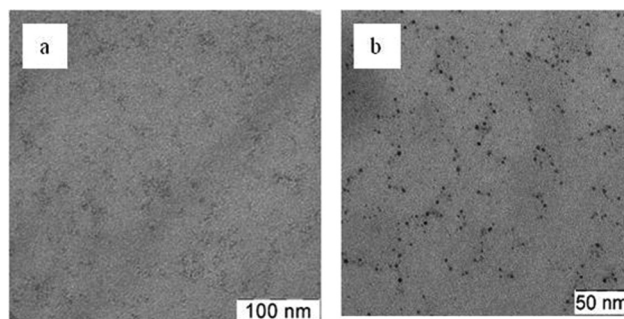


FIG. 1. TEM images of (a) deposited debris from ablated bulk Ag_2S and (b) deposited debris from ablated Ag_2S QDs.

scheme of heating nanosecond pulses and driving femtosecond pulses from different laser sources for HHG in plasmas. The ablation of QDs was carried out by nanosecond laser pulses (1064 nm, 5 ns, 10 Hz; Coherent, Q-Smart). An electronic delay between nanosecond and femtosecond pulses allowed us to apply sufficiently long delays between two pulses compared with the optical delay technique. The delay between pulses was tuned using an electronic delay generator (DG535; Stanford Research Systems). The synchronization of two laser sources, such as the most commonly used Ti:sapphire and Nd:YAG lasers, allows analyzing the enhancement of harmonics in the multiatomic particles produced during ablation of the bulk materials or of targets initially containing these multiatomic species. The main advantage of this approach is the control of the delay between the heating nanosecond pulses and the driving femtosecond pulses over a wide range between 0 and 10^5 ns, which is assumed to be sufficient for an analysis of the fast and slow components spreading out from the target in the laser-produced plasmas. The use of nanosecond Nd:YAG lasers as the sources of heating pulses may also offer some additional advantages compared with the commonly used picosecond pulses of the same repetition rate and wavelength as the driving sources. The application of nanosecond pulses to ablate the surface of targets allows the formation of less-ionized and less-excited plasma during longer periods of laser-matter interaction compared with picosecond pulses. This conclusion is based on the analysis of the nanosecond and picosecond ablation-induced plasma emission in the visible and extreme ultraviolet ranges in the case of the formation of the optimal plasmas leading to the generation of the highest harmonic yields. Different delays between heating and driving pulses from 5 to 20 000 ns were employed in present experiments, with the highest harmonic yield at ~ 200 ns.

The most important parameters during plasma HHG studies are the fluence of heating pulses and the intensity of driving pulses. The fluence of heating pulses on the surface of metal sulfide QD targets was varied between 1.5 and 3 J cm^{-2} depending on the used

samples. The difference in the optimal fluences allowing strongest emission of harmonics was attributed to different conditions of plasma formation in the case of the three used QD samples. The optimal fluence of nanosecond heating pulses in the case of ablation of bulk Ag_2S target was notably higher ($\sim 100 \text{ J cm}^{-2}$) due to a larger threshold of ablation of the solid sample compared with the gelatin containing quantum dots. The intensity of driving 800 nm pulses did not exceed $4 \times 10^{14} \text{ W cm}^{-2}$. Larger intensities of driving pulses caused strong plasma emission and a decrease of the harmonic yield, probably due to the appearance of a large amount of free electrons leading to a phase mismatch between the harmonic and driving waves. Stronger ablation fluences ($\sim 10 \text{ J cm}^{-2}$) caused the saturation of the harmonic yield, which was also followed by a modulation of the spectra of lower-order harmonics.

The harmonic emission was analyzed using an extreme ultraviolet spectrometer composed of a vertical slit, a gold-coated cylindrical mirror, a 1200 lines/mm flat field grating, a microchannel plate, and a CCD camera. The grating separated the harmonic orders by mapping the wavelength onto the horizontal axis of the microchannel plate and the CCD camera, which recorded the intensity of harmonics on the phosphor screen of the microchannel plate.

HHG in QDs was carried out using the single-color pump or the two-color pump of the laser-produced plasmas to determine the highest harmonic yield in different extreme ultraviolet ranges. For the two-color pump, the fundamental at 800 nm and its second harmonic were used. A 0.2 mm thick barium borate (BBO) crystal was installed inside the vacuum chamber into the path of the 800 nm radiation to generate the second harmonic [Fig. 2(a)]. The conversion efficiency of second harmonic pulses ($\lambda = 400 \text{ nm}$) was relatively small ($\sim 3\%$). Due to the small group velocity dispersion in the thin BBO crystal, the temporal overlap of the two driving pulses in the plasma area was sufficient for efficient generation of the odd and even harmonics in the longer-wavelength range of extreme ultraviolet. We analyzed the influence of this weak second orthogonally polarized field on the HHG in different QDs.

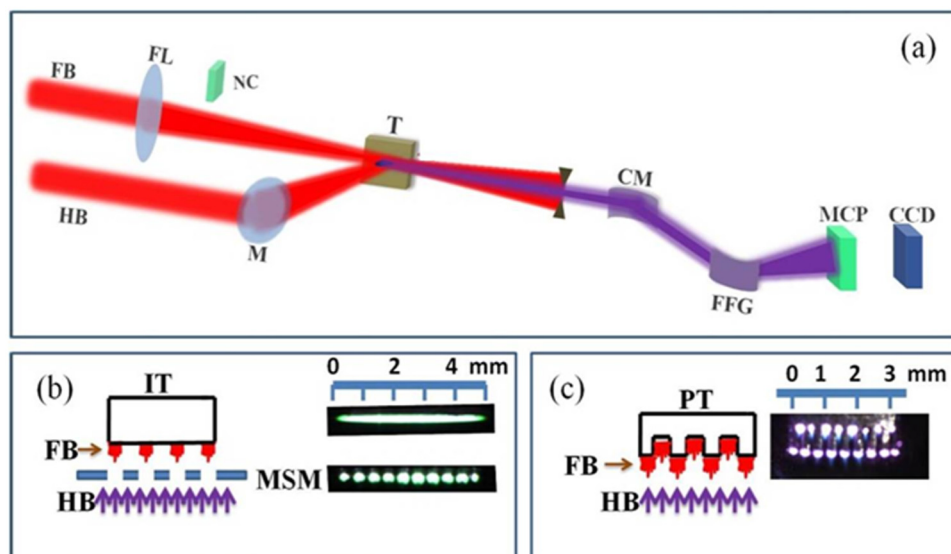


FIG. 2. (a) Experimental setup for HHG in laser-produced plasmas. FB, femtosecond beam; FL, focusing lens; NC, nonlinear crystal (BBO); HB, heating beam; M, mirror; T, target; CM, cylindrical mirror; FFG, flat field grating; MCP, microchannel plate; CCD, charge coupled device. (b) Formation of multi-jet plasma on the extended flat target. FB, femtosecond beam; HB, heating beam; IT, extended flat target; MSM, multislit mask. Insets: images of extended plasma (upper panel) and multi-jet plasma (bottom panel). (c) Formation of multi-jet plasma on the mechanically structured target. FB, femtosecond beam; HB, heating beam; PT, structured target. Inset: image of plasma jets from the structured target.

The formation of quasiphase matching for driving and harmonic waves in laser-produced plasmas was analyzed by variation of the morphology of extended QD-containing plasmas using spatially structured heating beams. To create heterogeneous spatial heating of targets, we used multislit masks installed in front of the targets, which allowed the formation of multijet plasmas containing different numbers of jets depending on the number of slits in the multislit mask [Fig. 2(b)].

We also used metal sulfide QD plates mechanically structured with steps of 0.3 mm distance, which were irradiated by a cylindrically focused heating pulse. The shape of such a target is shown in Fig. 2(c). The depth of the grooves of the Ag₂S QD- and Cd_{0.5}Zn_{0.5}S QD-containing surfaces was 2 mm. The plasma was formed on the upper and bottom parts of the target surface, as shown in the image of plasma jets. The driving pulse propagated through the plasma jets formed on the upper part of the target surface. The plasma jets formed on the bottom parts of the targets did not participate in the harmonic generation since they reach the axis of propagation of the driving beam only a few hundred nanoseconds after the beginning of the ablation when the femtosecond pulse has already passed through the plasma. This separation of the upper and bottom parts of the plasma jets has earlier allowed the formation of a nonlinear optical medium, which matches the requirements of quasiphase matching.

III. EXPERIMENTAL RESULTS

A. Single-color pump

Harmonic spectra from QDs were analyzed at different energies of driving 800-nm, 30-fs pulses. Figures 3(a) and 3(b) show

two groups of spectra generated in laser-produced plasmas containing Cd_{0.5}Zn_{0.5}S and CdS QDs. Both harmonic cutoff and intensity gradually increased with an increase of the 30 fs pulse energy from 0.3 to 0.93 mJ. The deviation of the growth of harmonic cutoff on the driving pulse energy from the relation predicted by the three-step model of HHG is attributed to the saturation of harmonic yield, which also affected and saturated the intensity dependence of low harmonics. The application of pure gelatin as the ablation target did not yield similar harmonic intensities as in the case of QD-containing targets, though some weak harmonics mostly attributed to the influence of carbon ions on the HHG process appeared in the long wavelength range of the extreme ultraviolet.

The application of two electronically separated pulses from different lasers synchronized by a digital delay generator allows analyzing the involvement of various multiparticle species in the HHG process. Particularly, one can expect the arrival of 3 nm particles in the region of the femtosecond laser beam propagation a few microseconds from the beginning of ablation. In the case of metal sulfide QD plasmas, an optimal delay around 150–250 ns yielded the highest harmonic intensity. Similar optimal delays were observed in the case of the ablation of bulk metal sulfides which produce single molecular species. Attempts to observe HHG at delays of up to 50 μ s, i.e., at the expected delay for thermalized larger nanoparticles, did not show any harmonic emission. Thus, the studies demonstrated that QDs arrive at the area of interaction with the femtosecond laser beam notably earlier than one would expect for a thermalized ablation plume. In other words, all metal sulfide particles ranging from single molecules to aggregates containing up to 10⁵ molecules acquire, from the very beginning, a similar velocity.

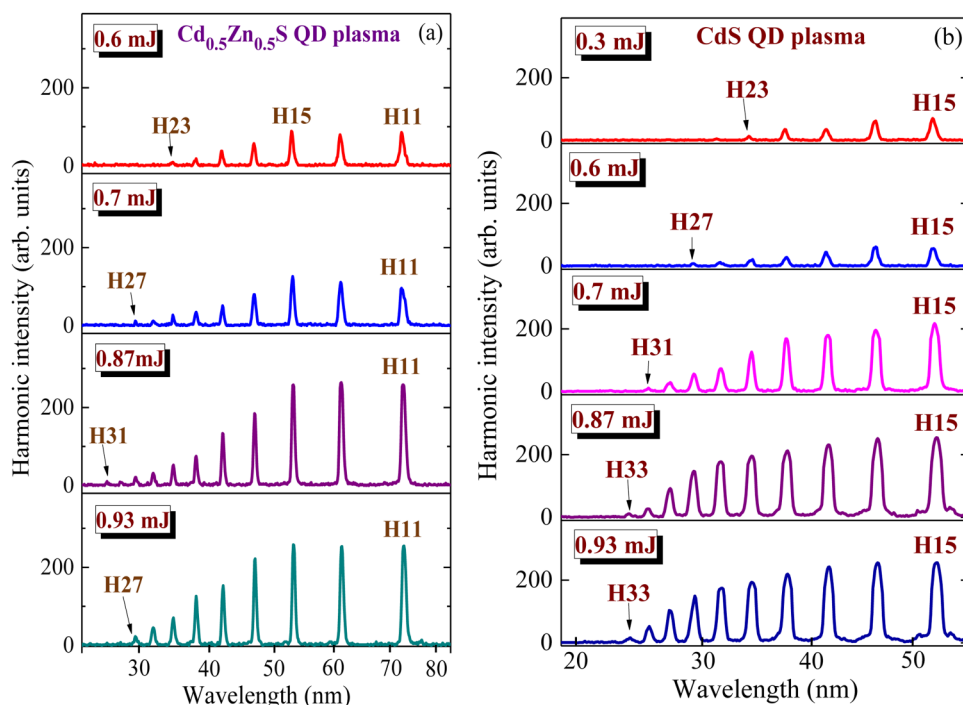


FIG. 3. Harmonic spectra from (a) Cd_{0.5}Zn_{0.5}S and (b) CdS QD plasmas measured at different energies of driving pulses.

An interesting feature of the metal sulfide QD-induced harmonic spectra is that, at stronger ablation, the spectral width of harmonics becomes two to three times broader compared with those generated in plasmas rich of monomolecular species of a similar material. The intensities of the ablation and driving pulses are crucial for optimizing the HHG from metal sulfide QDs. The 1.5- to 3-fold increase of the intensity of the driving pulse led to the insignificant extension of the harmonics (Fig. 3), which is a sign of HHG saturation in the medium. Moreover, at relatively high femtosecond laser intensities, we observed a decrease in the harmonic output, which can be ascribed to the phase mismatch as a result of higher free electron density. A similar phenomenon is observed when the ablation pulse on the surface of QD rich targets is increased above the optimal value for the harmonic generation. This reduction in harmonic intensity can be attributed to phenomena such as the fragmentation of QDs, an increase in free electron density, and self-defocusing, similarly to earlier observed saturation of HHG in the multiatomic systems like fullerenes. Another approach in harmonic modulation has earlier been demonstrated by controlling the chirp of the driving laser radiation in laser-gas jet experiments.²⁰ Moreover, the variations of harmonics and their “sharpness” were studied using a combination of the external control of the laser chirp and the intensity-induced variation of the laser chirp inside a nonlinear medium.²¹

The growth of the concentration of the harmonic emitters in the case of either QDs or single molecules plays an important role in the enhancement of HHG. The simplest way to achieve this is an increase of the heating pulse fluence, which in our case was performed by increasing the pulse energy at similar geometrical conditions of ablation. Saturation of the harmonic yield in some of these cases was followed by a modulation of the spectra of lower-order harmonics. Figure 4 shows the harmonics generated in the Ag₂S QD plasma formed at intensity $I = 2 \times 10^9 \text{ W cm}^{-2}$ of the nanosecond heating pulses, which was almost three times stronger than the one used at optimal conditions allowing the maximal yield of harmonics.

Such a variation of the harmonic spectrum was mostly determined by the modulation of the fundamental spectrum.

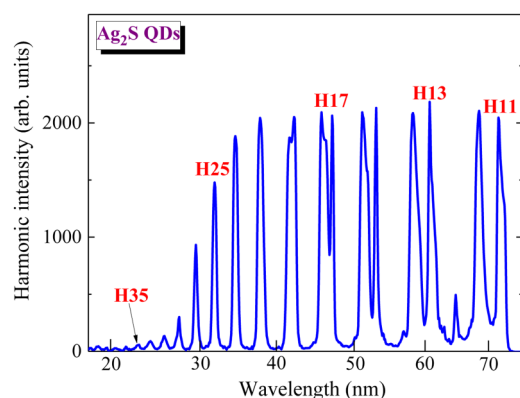


FIG. 4. HHG in the Ag₂S QD plasma formed at intensity $I = 2 \times 10^9 \text{ W cm}^{-2}$ of nanosecond heating pulses.

We observed a strong extension of the harmonic spectral distribution toward the blue side. One can see the notable modulation of the lower orders of harmonics (H11–H19). Each of these orders was separated into two parts, which led to the appearance of the strong lobes on the shorter-wavelength side. The decrease of the driving pulse intensity by the introduction of a positive and negative chirp in incompletely compressed pulses using the tuning of the grating in the compressor stage of our laser caused the disappearance of the modulation and broadening of harmonics. No significant influence of the self-phase modulation on the spectral distribution of harmonics was expected at these experimental conditions [relatively low density plasma ($3 \times 10^{17} \text{ cm}^{-3}$) and moderate laser intensities], which restrict the possibility of the influence of a strongly ionized medium on the phase characteristics of the driving and generating waves.

A highly ionized medium, with an electron density higher in the center than in the outer region, acts as a negative lens, leading to a defocusing of the laser beam in a plasma and hence to a reduction in the effective harmonic generation volume. In addition, the rapidly ionizing medium modifies the temporal structure of the femtosecond laser pulse. This process can be responsible for the broadening and splitting of the harmonics (Fig. 4).

The influence of the long trajectory of accelerated electrons in the laser-produced plasma can also play an important role in the appearance of different wavelength components of harmonic spectra. This process has been analyzed in Ref. 22. In the above paper, the images of harmonic distribution have demonstrated the components induced by long trajectories of electrons, which were clearly seen out of the axial line of harmonic distribution. Those measurements were taken at the conditions allowing the analysis of the divergence of harmonics. Notice the prevailing appearance of the longer-wavelength component of harmonics over the shorter-wavelength one. These signatures of different quantum paths show that rings attributed to long electron trajectory appear exclusively when the plasma is placed before the focus, in accordance with theoretical predictions discussed in Ref. 23 and experimental observations in gas HHG.^{24,25}

In our present studies, we did not observe the quantum path signatures like in above research. Notice that, contrary to the gases, the plasma medium containing neutrals, ions, and free electrons may influence the propagation of femtosecond pulse, especially in the case of the extended plume (5 mm), contrary to the commonly used narrow ($\sim 0.3 \text{ mm}$) gas and plasma jets. Free electrons naturally existing in the extended plasmas can diminish the role of the long trajectories of accelerated electrons, while the spectral splitting of propagating pulse can play an important role in the appearance of the short-wavelength components, especially in the case of lower-order harmonics. It is difficult to distinguish and separately analyze these two mechanisms of harmonic spectral modifications. Additional study is required to clarify the relative role of these two processes, which was not the goal of the present research. Notice that this topic has been partially analyzed in the above-refereed paper.²²

B. Two-color pump

Below, we address the two-color pump of QD plasma. The orthogonally polarized second field in the case of the two-color

pump participates in the modification of the trajectory of the accelerated electrons from being two-dimensional to three-dimensional, which may lead to a removal of the medium symmetry. This two-color pump-induced enhancement of harmonics has earlier been realized through the generation of 400 nm radiation in a separate channel with further mixing with 800 nm radiation in gases, as well as through the direct generation of the second harmonic in thin BBO crystals followed by focusing of two copropagating beams in gases and plasmas.^{26–28}

Here, we compare HHG in the case of the single-color pump (Fig. 5, upper panel) and the two-color pump (Fig. 5, bottom panel) using Ag₂S QDs. When applying a 0.4-mm thick BBO for the second harmonic generation (400 nm), some high-order harmonics (H12, H16, and H20) were notably weaker than other odd and even harmonics of the fundamental radiation due to insufficient temporal overlap of both waves in the plasma region. This heterogeneity in the harmonic intensity distribution was caused by the delay between 800 and 400 nm waves introduced by group velocity dispersion in BBO. The application of a thinner crystal (0.2 mm) allowed the generation of a relatively homogeneous intensity distribution of all harmonics, though the odd harmonics of 400-nm radiation were still stronger than other harmonics (Fig. 5, bottom panel), since even this thin crystal caused an ~40 fs delay between the maxima of the two 30 fs driving pulses. Correspondingly, the pulse overlap in the plasma region was relatively small.

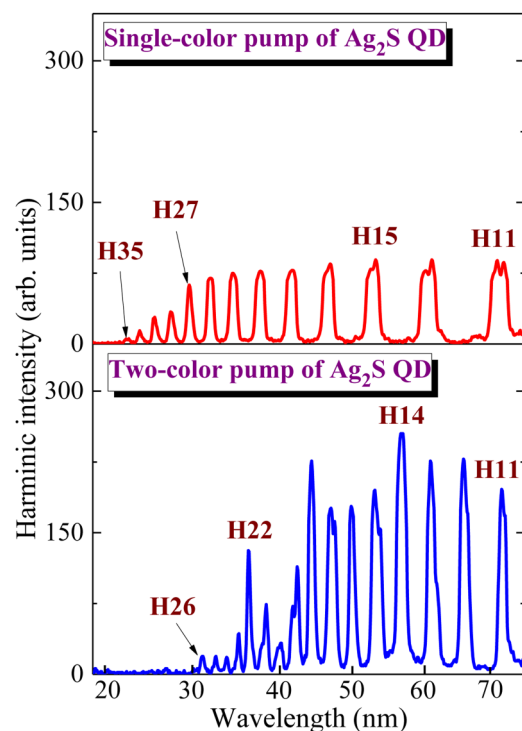


FIG. 5. Comparison of HHG in the case of (a) single-color pump and (b) two-color pump of Ag₂S QD laser-produced plasma using a 0.2 mm thick BBO.

Nevertheless, even this weak overlap of both 400 and 800 nm pulses rated as 1:30 by its energies was sufficient for a strong modification of the harmonic spectrum.

Two peculiarities were observed during these comparative studies. In the case of the two-color pump, the harmonic cutoff decreased compared with the single-color pump (H26 and H35, respectively, see bottom and upper panels of Fig. 5), probably due to the application of the shorter-wavelength component of the pumping radiation. In the case of the single-color pump, the harmonics were broadened and each of the lower orders had a shorter-wavelength component (upper panel) due to self-modulation of the driving pulse in the plasma region. Meanwhile, the harmonics in the two-color pump were spectrally narrower.

The insertion of the thin BBO crystal in the path of driving pulse led to some important changes in the plasma-laser interaction. The orthogonally polarized beam of second harmonic modifies the trajectory of the accelerated electron. Probably, the relatively weak second harmonic does not play an important role in the ionization dynamics. Thus, the modification of the trajectory of electrons, as well as the decrease of the role of longer trajectory in harmonic yield, causes the enhancement of the yield of harmonics at a relatively small addition of the second field. Since the joint influence of two trajectories of electrons may result in the broadening (and splitting) of the harmonic spectrum, the diminishing of the role of the long trajectory in the case of the two-color pump excludes, to some extent, this mechanism of harmonic broadening and splitting. In other words, the harmonics in two-color configuration become as narrow, as one can expect from the initial spectrum of the driving field.

Finally, it is worth noticing that the 3% conversion efficiency into the second harmonic in two-color pump experiments excludes its strong influence on ionization dynamics and suggests that the role of the second harmonic is a modification of electron trajectories during the HHG process, which can be considered as the main effect induced by the 400 nm field.

C. Structured plasma

Below, we address HHG in spatially structured plasmas containing metal sulfide QDs for the realization of quasiphase matching between the driving and harmonic waves. This concept may successfully be applied when the absorption of generated harmonics in the extreme ultraviolet region is small compared to the enhancement of this radiation due to quasiphase matching. Quasiphase matching has previously been demonstrated in gaseous^{29,30} and plasma¹⁷ media. One of the approaches here is the division of an extended medium into groups of narrow media separated by vacuum. In these parts, the conditions of harmonics enhancement are maintained along the whole coherence length, i.e., until the phase difference $\Delta\varphi$ between converting and converted waves becomes equal to π .

In the case of laser-produced plasmas produced on the surfaces of bulk metals (Ag, In, etc.), the conditions of quasiphase matching are determined by the presence of a suitable concentration of free electrons in a single jet of multi-jet plasmas. One can expect the fulfillment of the basic rule for quasiphase matching at the conditions when the plasma dispersion assumes to be a dominant mechanism of phase mismatch, which stipulates the

relation between the jet sizes and maximally enhanced harmonic ($H_{\text{qpm}} \times l_{\text{jet}} \propto \text{const}$). The ablation of bulk materials with spatially structured heating pulse allows the formation of spatially structured plasma where the boundaries of jets distinguish the areas of the presence and absence of electrons. This difference in electron concentrations inside the plasma jet and the interjet space allows the formation of quasiphase matching for the group of harmonics and the driving radiation.

The results presented in Fig. 6(a) show the formation of quasiphase matching conditions in the case of Ag_2S bulk target ablation via multislit mask. One can clearly see a difference in the envelopes of the harmonics distribution in the cases of an extended flat (upper panel) and spatially structured plasma (lower two panels). An enhancement of higher orders in the case of multijet plasmas compared to the extended flat plasma is observed. Notice that higher harmonics, i.e., those above the 33rd order, were barely seen in the case of the extended plasma. The enhancement factor of H41 in the case of multijet plasmas was calculated to be close to 30 \times . Another important feature of this process in the case of multijet plasmas produced on the surface of a bulk material is the relatively narrow envelope of the group of enhanced harmonics comprising nine harmonic orders (H25–H41, lowest panel).

A similar extreme ultraviolet intensity pattern appeared in the case of the ablation of the mixture of $\text{Cd}_{0.5}\text{Zn}_{0.5}\text{S}$ QDs [see scheme shown in Fig. 2(b)] and gelatin with and without the application of multislit mask [Fig. 6(b)]. Ablation of such targets at a relatively high fluence allowing the formation of dense plasma probably did not follow with the presence of a large amount of free electrons. Another reason for the diminished role of quasiphase matching in the former case is the observation of lower cutoff with regard to the ablated bulk Ag_2S . Quasiphase matching in plasmas differs from the plateaulike distribution of harmonics mostly when the

constituents of the plasma allow the generation of harmonic orders greater than 40 or even 50. In the meantime, the studied QDs did not demonstrate the extended cutoff harmonics, thus diminishing the chances in the formation of quasiphase matching conditions [compare the dashed-dotted curve of Fig. 6(b) and the middle panel of Fig. 6(a)].

The scheme of quasiphase matching where the driving femto-second beam interacts only with the top surface of a mechanically structured target [Fig. 2(c)] did not show a modulation of the intensity envelope of the generated harmonics similar to the one presented in Fig. 6(b). Though the conditions of laser-produced plasma modulation were preserved for the propagating beam, the phase modulation between driving and harmonic waves was insufficient to allow quasiphase matching in the shorter-wavelength region of the extreme ultraviolet, probably due to the influence of free electrons appearing in the area between plasma jets.

IV. DISCUSSION

The interaction of multiparticle species with a strong laser field was first analyzed in the media comprising the clusters containing a few thousands of atoms of noble gases.^{1,2,9} The theoretical concepts describing the models of interaction of such structures possessing specific properties with the laser pump were analyzed in Refs. 8 and 31–34. The specific properties of clusters, quantum dots, and nanoparticles refer to those which allow achieving the enhanced yield of harmonics from the multiparticle medium compared with a monomer containing medium. In the case of gas clusters, those include the involvement of different channels of harmonic generation, particularly, the ionization and recombination to the same ion of the cluster, to the neighboring ions, and to the whole cluster.⁹ These processes differ from the case of atoms

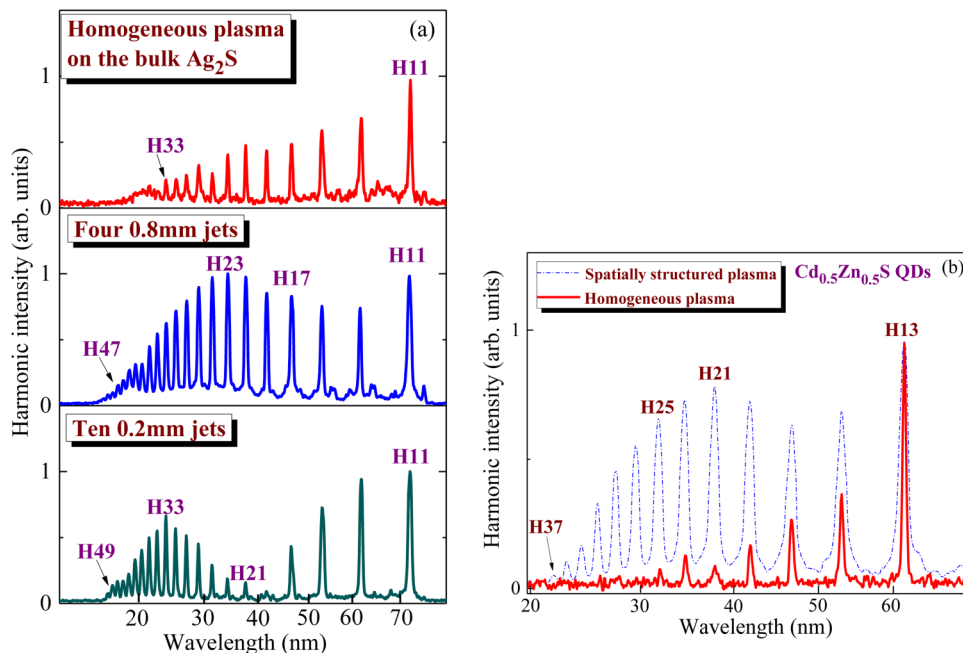


FIG. 6. Comparison of quasiphase matching in the case of ablation of (a) bulk (Ag_2S) and (b) QD ($\text{Cd}_{0.5}\text{Zn}_{0.5}\text{S}$) targets. (a) Upper panel shows the gradually decreased harmonics from extended plasma produced on the surface of bulk Ag_2S target. Application of multislit masks with different sizes of slits (0.8 and 0.2 mm) led to the generation of the groups of enhanced harmonics centered at around H23 (middle panel) and H33 (bottom panel). (b) Solid curve shows the gradually decreased harmonic spectrum in the case of extended plasma produced on the target containing $\text{Cd}_{0.5}\text{Zn}_{0.5}\text{S}$ QDs. Dashed-dotted curve demonstrates the quasiphase matching conditions for the group of harmonics at around H21 in the case of four 0.8 mm long jets.

and may either enhance or diminish the high-order nonlinear optical response of the medium depending on the sizes of nanoparticles. Meanwhile, the enhanced cross section of the recombination of the accelerated electron and parent particle may naturally lead to the growth of the harmonic yield. In the case of significantly larger parent particles containing thousands to millions of atoms, the larger sizes of former species decrease the probability of missing the interaction with the accelerated electron, which returns during the second half of cycle toward the emitters of electrons. In other words, large sizes of parent particles allow capturing the returning electron with higher probability. However, there are some limits in this concept, which point out the existence of an optimal size of multiparticles associated with the maximal yield of harmonic emission.

The main advantage of the HHG in laser-produced plasmas from QDs is the higher efficiency compared to a gas jet and a bulk target. We analyzed the harmonic generation efficiency in the case of ablated CdS bulk plate, CdS QDs, as well as compared them with HHG from argon gas. The details of the comparative HHG experiments using gas and plasma from metal targets are described elsewhere.³⁵ Those studies have demonstrated a 3- to 5-fold stronger harmonic yield in the latter case. Our present experiments using metal sulfide-containing plasmas also showed a stronger harmonic yield from ablated CdS and CdS QD targets compared to the argon gas at similar concentrations of gas and plasma media. These comparative experiments were carried out using a narrow gas flow from a stainless steel needle with an inner diameter of 0.3 mm and the CdS and CdS QD plasma plumes of the sizes of 0.3 mm at similar energies of the driving pulses. We observed the 4× (in the case of ablated bulk CdS) and 10× (in the case of ablated CdS QDs) prevalence of the conversion efficiency from plasma media compared with the gas medium at similar conditions of experiments.

The experimental HHG studies of multiparticle gaseous and plasma systems,^{1,2,9,36,37} as well as the theoretical consideration of the HHG process in clustered media^{31–34} have shown the advantages of these species for HHG. Those studies used the single-color laser pulses for the harmonic generation. Earlier, the two-color pump concept in multiparticle systems has been realized, to the best of our knowledge, only in the case of plasma HHG.^{7,38} Our present studies provide further steps in applications of the two-color pump for the analysis of the interaction of two orthogonally polarized waves at a suitable overlap of 800 and 400 nm pulses in QD plasma.

Ablation by nanosecond laser pulse most probably would lead to some disintegration of QDs due to avalanche ionization and Joule heating, leading to the presence of both QDs and single molecular species in the plasma plume. It is not clear if HHG solely happens from neutral QDs and nanoparticles/clusters generated due to ablation or it happens in charged species and ions. The electron density of such plasmas has never been measured. The work function for CdS QDs is about 5.2 eV.³⁹ For Ti:sapphire laser pulses at 800 nm wavelength and the energy of quanta 1.55 eV, this would mean essentially four-photon ionization.

Most probably, HHG in that case can be considered as a sum of harmonic emission from different emitters. To study the integrity of QDs in the plasma plume, we optimized the plasma

conditions for maximal harmonic yield using the CdS QD target. Then, we deposited the plasma debris on a fused silica substrate placed near the target. The TEM analysis of debris showed that the deposition contains the QDs with approximately the same sizes as the original species [Fig. 1(b)]. This result suggests that, for the low-excitation regime of plasma formation (i.e., for heating pulse intensity of about $8 \times 10^8 \text{ W cm}^{-2}$), the ablated QDs keep their morphology within the plasma until the intense femtosecond pump arrives in the area of interaction.

Our observations give a rough pattern of the ablation and HHG from QD targets. The material around the QDs is a dried gelatin, which has a lower ablation threshold than metal sulfide materials. Therefore, the gelatin starts to ablate at relatively low intensities, carrying QDs with it, resulting in the lower heating pulse intensity required for the ablation and evaporation of the target. We found that the HHG from metal sulfide multiatomic particles started to be efficient at considerably smaller heating pulse intensities [$(3\text{--}6) \times 10^8 \text{ W cm}^{-2}$] compared with the case of bulk metal sulfides [$(1\text{--}3) \times 10^{10} \text{ W cm}^{-2}$]. This range of optimal intensities [$(3\text{--}6) \times 10^8 \text{ W cm}^{-2}$] corresponds to a fluence of $1.5\text{--}3 \text{ J cm}^{-2}$ in the case of 5 ns pulses. The spectrum broadening and splitting is observed at a fluence of 10 J cm^{-2} (Fig. 4), which corresponds to an intensity of $2 \times 10^9 \text{ W cm}^{-2}$ for 5 ns heating pulses.

Our studies showed the modulation of the lower orders of harmonics leading to the formation of the blue-shifted components. This process can be attributed to the self-phase modulation and chirping of the fundamental radiation propagating through the dense nonlinear medium. The decrease of the driving pulse intensity significantly lowered the modulation of harmonic spectra. The plasma density was estimated to be $3 \times 10^{17} \text{ cm}^{-3}$. Usually, self-phase modulation is related to a nonlinear response of the neutral medium. Once we assume ionization nonlinearity originating from the highly nonlinear field ionization process, then this type of nonlinear interaction will lead first of all to a strong blue shift in the spectrum of the laser pulse. Meanwhile, the interesting structure of the spectrum in Fig. 4 is unlikely to be explained just by self-phase modulation induced by propagating driving pulses and plasma dispersion. Further studies require for determining the origin of such modulation of generating spectra. For example, the measurement of the spectrum of the transmitted fundamental pulse would unequivocally determine the relative role of self-phase modulation and ionization nonlinearity in the HHG spectrum evolution.

The process of harmonic broadening and splitting most often was reported as a consequence of using driving pulses possessing intensities above some threshold level. This effect has been frequently reported during gas HHG studies.^{20,21} Similar broadening and splitting caused by the application of strong driving laser intensity has been reported during plasma HHG studies as well.^{40,41} The analysis of self-interaction during HHG has been presented in Ref. 42. Meanwhile, plasma plume is a specific and more sophisticated target than gas, which initially possesses some amount of free electrons, which themselves may cause the modulation of the harmonic spectrum. This means that the spectral features of HHG depend not only on the intensity of the driving pulses but also on the intensity of heating pulses. Our observations of strong modulation and splitting of lower-order harmonics confirm this assumption.

The ability of the heating of semiconductor QDs due to one-photon absorption of the second harmonic of the pump laser radiation was insignificant due to the low density of the plasma plume. Notice that almost no harmonics were generated in the case of pure gelatin ablation at similar conditions of HHG experiments. We observed only a few extremely weak lowest order harmonics from the gelatin plasma at relatively strong ablation conditions (i.e., at the heating pulse intensity of $3 \times 10^{10} \text{ W cm}^{-2}$). The harmonic generation efficiency in that case was calculated to be not more than 6×10^{-7} , while the same parameter in the case of QD-contained plasmas was almost two orders of magnitude larger (4×10^{-5}).

The quasiphase-matched HHG is a coherent nonlinear process. To prove the realization of quasiphase matching in the experiments, one has to show the dependences of the HHG efficiency on the length of the structured laser-produced plasmas. We did not carry out these studies in the case of QD laser-produced plasmas, while similar studies of the quasiphase matching in the plasmas produced from bulk targets have revealed the quadratic dependence of the harmonic yield on the number of plasma jets.⁴³

The quasiphase matching concept used in the present paper broadens the range of applications of the specific relations between the fundamental wave and the waves of harmonics in different regions of the extreme ultraviolet. The basics of this concept were initially demonstrated in the case of gas media and further developed during the last few years while using the plasma plumes. The crucial point for the realization of quasiphase matching in the latter medium is a formation of such a plasma configuration that allows the manipulation between the phases of the group of harmonics and fundamental radiation, leading to the tuning of the phase matching between them during propagation through the group of the plasma jets possessing variable spatial modulation. One of the most useful techniques to form such conditions is the separation of the extended plasma produced during focusing of the heating pulse by a cylindrical lens into a group of equidistant plasma jets. Such multijet plasma allows a significant enhancement of a group of harmonics, while other harmonics become suppressed. Another method of multijet plasma formation is the application of the perforated ablating target. The detailed description of these two methods can be found elsewhere.^{17,44}

Our studies show that spatially modulated plasma containing quantum dots can also be considered as the efficient medium for the demonstration of the quasiphase matching concept [Fig. 6(b)]. The enhancement of harmonics exceeding a factor of 10, especially for those above the 25th order (compare the dotted and solid curves in this spectral range), clearly points out the decisive role of the optimized relation between the phases of those harmonics and the driving pulse propagating through the QD-containing plasma. Notice that neither strong harmonics nor quasiphase matching effect was observed in the case of the ablation of the pure gelatin.

The concepts of plasma high-order harmonic generation in laser-produced plasmas, quasiphase matching in multijet plasma, two-color pump of plasma, and harmonic enhancement in nanoparticle/quantum dot plasmas are not new. However, it is the first time when all those concepts of the amendment of harmonic generation from QDs were combined in a single set of studies. The physics behind the observed difference of harmonic emission from monomers and multiparticle associates is as follows. Stronger

harmonic flux from QDs with regard to the monomers could be attributed to better conditions of the recombination of accelerated electrons with harmonic emitters in the case of metal sulfide QDs ablation and spreading, as well as to specific properties of QDs, which, as was mentioned, include the ionization and recombination to the same ion of the cluster, to the neighboring ions, and to the whole cluster. The theoretical justification of utilizing the plasmonic fields in some multiparticle systems for the generation of efficient coherent extreme ultraviolet radiation has been reported in Ref. 45. The effectiveness of HHG in the presence of such structures can be attributed to the plasmonic properties of nanoparticles and quantum dots leading to the involvement of the local fields in the enhancement of the nonlinear optical response of the medium. Particularly, plasmon-enhanced high-harmonic generation from silicon was reported in Ref. 46. The authors proposed that the field can become strong enough to convert the fundamental laser frequency into high-order harmonics through an extremely nonlinear interaction with gas atoms that occupy the nanoscopic volume surrounding the nanoantennas. One can assume that a similar process can play an important role in the case of metal sulfide and alloyed QDs studied here.

One can assume that quantum dots are the small-sized nanoparticles, which at specific conditions of excitation can demonstrate the quantum effect when local fields can enhance the nonlinear optical response of the medium. The comparison of HHG using QDs and nanoparticles of the same elemental consistency is a straightforward way to judge about the role of the quantum effect. However, these comparative experiments can be barely realized due to experimental obstacles. The synthesis of larger-sized metal sulfide structures was problematic due to sedimentation prior to the aggregation of the large particles ($>10 \text{ nm}$). Meanwhile, our synthesized particles had the sizes of 2–3 nm, which ideally matched the appearance of the structures allowing an observation of the quantum properties and local field enhancement. Thus, one can expect an influence of these processes on the HHG during our experiments.

There are still a lot of issues that have to be clarified in the case of the application of the used QDs for HHG. It remains a puzzle how the chemical composition, crystal structure, and spatial scales of the QDs affect the HHG efficiency and the cutoff frequency. There remain also other questions regarding the charge state of this plasma medium, which could be resolved only by using time-of-flight mass spectrometry. Particularly, are the QDs charged before the pump pulse comes? How many electrons are ionized under the high intensity pump pulse from each QD? What are the exact ionization potentials of the chosen QDs and how do they affect the HHG cutoff?

V. CONCLUSIONS

We have reported high-order harmonics generation in the laser-produced plasmas containing quantum dots of metal sulfides using different approaches. We have analyzed the harmonic generation during the propagation of 800 nm, 30 fs pulses through the plasmas containing Ag_2S , CdS , and $\text{Cd}_{0.5}\text{Zn}_{0.5}\text{S}$ QDs. The self-phase modulation of lower-order harmonics and an intensity-dependent saturation of the harmonic yield were discussed. The application of two-color pumping allowed the generation of almost equal odd and even harmonics using a 0.2-mm thick barium

borate crystal, while the application of a thicker (0.4 mm) crystal for second harmonic generation caused a weaker temporal overlap of the two driving fields (800 and 400 nm) in the metal sulfide QD plasma area. Finally, the studies of quasiphase matching conditions in spatially structured plasmas produced by either structuring the heating beam or the surface of the ablating target showed the formation of a group of enhanced shorter-wavelength harmonics, though this process was less pronounced compared to the formation of a structured plasma on the surface of bulk metal sulfides.

ACKNOWLEDGMENTS

This research was supported by the National Key Research and Development Program of China (Nos. 2017YFB1104700 and 2018YFB1107202), the National Natural Science Foundation of China (NNSFC) (Nos. 91750205, 61774155, and 61705227), the Bill & Melinda Gates Foundation of the US (No. OPP1157723), the Scientific Research Project of the Chinese Academy of Sciences (No. QYZDB-SSW-SYS038), the Jilin Provincial Science & Technology Development Project (No. 20180414019GH), and the Key Program of the International Partnership Program of CAS (No. 181722KYSB20160015). R.A.G., O.V.O., A.I.Z., and M.S.S. acknowledge support from the Russian Foundation for Basic Research (RFBR) (No. 17-52-12034 ННЮ_а). M.W. and H.Z. acknowledge support from the German Science Foundation (DFG) (No. ZA 110/28-1).

REFERENCES

- ¹T. D. Donnelly, T. Ditmire, K. Neuman, M. D. Perry, and R. W. Falcone, *Phys. Rev. Lett.* **76**, 2472 (1996).
- ²C. Vozzi, M. Nisoli, J.-P. Caumes, G. Sansone, S. Stagira, S. De Silvestri, M. Vecchiocattivi, D. Bassi, M. Pascolini, L. Poletto, P. Villorosi, and G. Tondello, *Appl. Phys. Lett.* **86**, 111121 (2005).
- ³R. A. Ganeev, P. A. Naik, H. Singhal, J. A. Chakera, M. Kumar, M. P. Joshi, A. K. Srivastava, and P. D. Gupta, *Phys. Rev. A* **83**, 013820 (2011).
- ⁴R. A. Ganeev, M. Baba, M. Morita, D. Rau, H. Fujii, A. I. Ryasnyansky, N. Ishizawa, M. Suzuki, and H. Kuroda, *J. Opt. A* **6**, 447 (2004).
- ⁵R. A. Ganeev, M. Suzuki, M. Baba, M. Ichihara, and H. Kuroda, *J. Phys. B* **41**, 045603 (2008).
- ⁶H. Singhal, R. A. Ganeev, P. A. Naik, J. A. Chakera, U. Chakravarty, H. S. Vora, A. K. Srivastava, C. Mukherjee, C. P. Navathe, S. K. Deb, and P. D. Gupta, *Phys. Rev. A* **82**, 043821 (2010).
- ⁷R. A. Ganeev, G. S. Boltaev, V. V. Kim, K. Zhang, A. I. Zvyagin, M. S. Smirnov, O. V. Ovchinnikov, P. V. Redkin, M. Wöstmann, H. Zacharias, and C. Guo, *Opt. Express* **26**, 35013 (2018).
- ⁸J. R. Vázquez de Aldana and L. Roso, *J. Opt. Soc. Am. B* **18**, 325 (2001).
- ⁹H. Ruf, C. Handschin, R. Cireasa, N. Thiré, A. Ferré, S. Petit, D. Descamps, E. Mével, E. Constant, V. Blanchet, B. Fabre, and Y. Mairesse, *Phys. Rev. Lett.* **110**, 083902 (2013).
- ¹⁰H. Singhal, V. Arora, B. S. Rao, P. A. Naik, U. Chakravarty, R. A. Khan, and P. D. Gupta, *Phys. Rev. A* **79**, 023807 (2009).
- ¹¹R. A. Ganeev, V. V. Strelkov, C. Hutchison, A. Zaïr, D. Kilbane, M. A. Khokhlova, and J. P. Marangos, *Phys. Rev. A* **85**, 023832 (2012).
- ¹²R. A. Ganeev, *High-Order Harmonic Generation in Laser Plasma Plumes* (Imperial College Press, London, 2012).
- ¹³Y. Pertot, S. Chen, S. D. Khan, L. B. Elouga Bom, T. Ozaki, and Z. Chang, *J. Phys. B* **45**, 074017 (2012).
- ¹⁴S. Haessler, V. Strelkov, L. B. Elouga Bom, M. Khokhlova, O. Gobert, J.-F. Hergott, F. Lepetit, M. Perdrix, T. Ozaki, and P. Salières, *New J. Phys.* **15**, 013051 (2013).
- ¹⁵N. Rosenthal and G. Marcus, *Phys. Rev. Lett.* **115**, 133901 (2015).
- ¹⁶M. A. Fareed, V. V. Strelkov, N. Thiré, S. Mondal, B. E. Schmidt, F. Légaré, and T. Ozaki, *Nat. Commun.* **8**, 16061 (2017).
- ¹⁷M. Wöstmann, L. Splithoff, and H. Zacharias, *Opt. Express* **26**, 14524 (2018).
- ¹⁸Z. Abdelrahman, M. A. Khokhlova, D. J. Walke, T. Witting, A. Zaïr, V. V. Strelkov, J. P. Marangos, and J. W. G. Tisch, *Opt. Express* **26**, 15745 (2018).
- ¹⁹M. A. Fareed, V. V. Strelkov, M. Singh, N. Thiré, S. Mondal, B. E. Schmidt, F. Légaré, and T. Ozaki, *Phys. Rev. Lett.* **121**, 023201 (2018).
- ²⁰H. T. Kim, I. J. Kim, D. G. Lee, K.-H. Hong, Y. S. Lee, V. Tosa, and C. H. Nam, *Phys. Rev. A* **69**, 031805 (2004).
- ²¹H. T. Kim, D. G. Lee, K.-H. Hong, J.-H. Kim, I. W. Choi, and C. H. Nam, *Phys. Rev. A* **67**, 051801 (2003).
- ²²R. A. Ganeev, C. Hutchison, T. Siegel, A. Zaïr, and J. P. Marangos, *Phys. Rev. A* **83**, 063837 (2011).
- ²³M. B. Gaarde, F. Salin, E. Constant, P. Balcou, K. J. Schafer, K. C. Kulander, and A. L'Huillier, *Phys. Rev. A* **59**, 1367 (1999).
- ²⁴A. Zaïr, M. Holler, A. Guandalini, F. Schapper, J. Biegert, L. Gallmann, U. Keller, A. S. Wyatt, A. Monmayrant, I. A. Walmsley, E. Cormier, T. Augustine, J. P. Caumes, and P. Salières, *Phys. Rev. Lett.* **100**, 143902 (2008).
- ²⁵M. Holler, A. Zaïr, F. Schapper, T. Augustine, E. Cormier, A. Wyatt, A. Monmayrant, I. A. Walmsley, L. Gallmann, P. Salières, and U. Keller, *Opt. Express* **17**, 5716 (2009).
- ²⁶I. J. Kim, C. M. Kim, H. T. Kim, G. H. Lee, Y. S. Lee, J. Y. Park, D. J. Cho, and C. H. Nam, *Phys. Rev. Lett.* **94**, 243901 (2005).
- ²⁷J. Mauritsson, P. Johnsson, E. Gustafsson, A. L'Huillier, K. J. Schafer, and M. B. Gaarde, *Phys. Rev. Lett.* **97**, 013001 (2006).
- ²⁸R. A. Ganeev, H. Singhal, P. A. Naik, I. A. Kulagin, P. V. Redkin, J. A. Chakera, M. Tayyab, R. A. Khan, and P. D. Gupta, *Phys. Rev. A* **80**, 033845 (2009).
- ²⁹J. Seres, V. S. Yakovlev, E. Seres, Ch. Streli, P. Wobrowschek, Ch. Spielmann, and F. Krausz, *Nat. Phys.* **3**, 878 (2007).
- ³⁰A. Pirri, C. Corsi, and M. Bellini, *Phys. Rev. A* **78**, 011801 (2008).
- ³¹S. X. Hu and Z. Z. Xu, *Appl. Phys. Lett.* **71**, 2605 (1997).
- ³²V. Vénier, R. Taïeb, and A. Maquet, *Phys. Rev. A* **65**, 013202 (2001).
- ³³T. Tajima, Y. Kishimoto, and M. C. Downer, *Phys. Plasmas* **6**, 3759 (1999).
- ³⁴J. W. G. Tisch, *Phys. Rev. A* **62**, 041802 (2000).
- ³⁵R. A. Ganeev, G. S. Boltaev, V. V. Kim, M. Venkatesh, and C. Guo, *OSA Continuum* **2**, 2381 (2019).
- ³⁶R. A. Ganeev, M. Baba, M. Suzuki, and H. Kuroda, *J. Phys. B* **47**, 135401 (2014).
- ³⁷M. Wöstmann, P. V. Redkin, J. Zheng, H. Witte, R. A. Ganeev, and H. Zacharias, *Appl. Phys. B* **120**, 17 (2015).
- ³⁸R. A. Ganeev, M. Suzuki, and H. Kuroda, *Eur. Phys. J. D* **70**, 21 (2016).
- ³⁹P. Kulis, J. Butikova, B. Polyakov, G. Marcins, J. Pervenecka, K. Pudzs, and I. Tale, *IOP Conf. Ser.* **38**, 012048 (2012).
- ⁴⁰L. B. Elouga Bom, J.-C. Kieffer, R. A. Ganeev, M. Suzuki, H. Kuroda, and T. Ozaki, *Phys. Rev. A* **75**, 033804 (2007).
- ⁴¹R. A. Ganeev, L. B. Elouga Bom, M. C. H. Wong, J.-P. Brichta, V. R. Bhardwaj, P. V. Redkin, and T. Ozaki, *Phys. Rev. A* **80**, 043808 (2009).
- ⁴²R. A. Ganeev, M. Suzuki, M. Baba, and H. Kuroda, *J. Opt. Soc. Am. B* **23**, 1332 (2006).
- ⁴³R. A. Ganeev, V. Tosa, K. Kovács, M. Suzuki, S. Yoneya, and H. Kuroda, *Phys. Rev. A* **91**, 043823 (2015).
- ⁴⁴R. A. Ganeev, M. Suzuki, and H. Kuroda, *Phys. Rev. A* **89**, 033821 (2014).
- ⁴⁵Y.-Y. Yang, A. Scrinzi, A. Husakou, Q.-G. Li, S. L. Strebings, F. Süßmann, H.-J. Yu, S. Kim, E. Rühl, J. Herrmann, X.-C. Lin, and M. F. Kling, *Opt. Express* **21**, 2195 (2013).
- ⁴⁶G. Vampa, B. G. Ghamsari, S. Siadat Mousavi, T. J. Hammond, A. Olivieri, E. Lisicka-Skre, A. Yu. Naumov, D. M. Villeneuve, A. Staudte, P. Berini, and P. B. Corkum, *Nat. Phys.* **13**, 659 (2017).